Original geometrical stopping criteria associated to multilevel adaptive mesh refinement for problems with local singularities

Isabelle Ramière, Hao Liu, Frédéric Lebon

▶ **To cite this version:**

Isabelle Ramière, Hao Liu, Frédéric Lebon. Original geometrical stopping criteria associated to multilevel adaptive mesh refinement for problems with local singularities. Computational Mechanics, 2019, 64 (3), pp.645-661. ⟨10.1007/s00466-019-01674-7⟩. ⟨hal-02336644⟩

HAL Id: hal-02336644

https://hal.science/hal-02336644v1

Submitted on 29 Nov 2019

HAL is a multi-disciplinary open access archive for the deposit and dissemination of scientific research documents, whether they are published or not. The documents may come from teaching and research institutions in France or abroad, or from public or private research centers.

L'archive ouverte pluridisciplinaire **HAL**, est destinée au dépôt et à la diffusion de documents scientifiques de niveau recherche, publiés ou non, émanant des établissements d'enseignement et de recherche français ou étrangers, des laboratoires publics ou privés.

HAL Authorization

Original geometrical stopping criteria associated to multilevel adaptive mesh refinement for problems with local singularities

Isabelle Ramière[1] · Hao Liu[1] · Frédéric Lebon[2]

Abstract
This paper introduces a local multilevel mesh refinement strategy that automatically stops relating to a user-defined tolerance even in case of local singular solutions. Refinement levels are automatically generated thanks to a criterion based on the direct comparison of the a posteriori error estimate with the local prescribed error. Singular solutions locally increase with the mesh step (e.g. load discontinuities, point load or geometric induced singularities) and are hence characterized by locally large element-wise error whatever the mesh refinement. Then, the refinement criterion may not be self-sufficient to stop the refinement process. Additional stopping criteria are required if no physical-designed estimator wants to be used. Two original geometry-based stopping criteria are proposed that consist in automatically determining the critical region for which the mesh refinement becomes inefficient. Numerical examples show the efficiency of the methodology for stress tensor approximation in L^2-relative or L^∞-absolute norms.

Keywords Adaptive mesh refinement · Local Defect Correction method · A posteriori error estimator · Stopping criteria · Local singular solution · Elastostatics

1 Introduction

Since the 80's, adaptive mesh refinement techniques are commonly used to locally improve the solutions of ordinary or partial differential equations, see for example [5,7–9,15, 20,25,42] and the references therein. Such locally refined meshes are generally obtained thanks to an iterative process based on a posteriori error estimators [3,39,43]. Either quantitative or qualitative use of the error estimator is generally made. In the first category, a direct comparison of the error estimator with the user prescribed accuracy (e.g. [14,17]) is conducted. In the second category, the detected zone is usually defined as the union of the elements for which the error estimator is greater than a proportion of the maximal estimated error (e.g. [16,21]). The second methodology has the main drawback to be not related to the user prescribed accuracy. Moreover it has been shown in [4] that the optimal proportion seems to depend on the problem. While the refinement criteria are generally well analyzed in the literature, stopping criteria are poorly studied although they play an important role in the obtained results.

Again, the way to stop the refinement process is non-unique. The most used approach seems to consist in checking at each refinement iteration if the estimated error is less than the prescribed accuracy (e.g. [14,17]). This stopping criterion approach is strongly related to the convergence of the error estimator [22,31], as confirm the numerical examples provided in [28]. Other classical techniques consist in stopping the refinement process thanks to a priori given parameters independent of the prescribed error : number of iterations (e.g. [2,21]), minimal number of elements to refined [4], etc. Various stopping criteria are often combined in order to optimize the refinement strategy, see for example [13,32].

A singular solution can be defined as a solution field that does not converge towards a specific value at a point (or edge) of the domain, named singularity. Hence, while locally refining the mesh, the absolute value of the solution at this singularity keeps increasing. According to the Saint Venant's Principle [6], the Finite Element approximation is

✉ Isabelle Ramière
isabelle.ramiere@cea.fr

Frédéric Lebon
lebon@lma.cnrs-mrs.fr

[1] CEA, DEN, DEC, SESC, LSC, 13108 Saint-Paul Lez Durance, France

[2] CNRS, Centrale Marseille, LMA, Aix-Marseille University, 13453 Marseille cedex 13, France

fine at some distance away from the singularity but is polluted near the singularity. In many industrial software, it is recommended to ignore the singularities if the user is only interested by the solution far away from any singularities or by integrals of the solutions over the singularity region. On the contrary, the mesh must be locally refined in order to capture the singularity effect. In this latter case, only stopping criteria based on a priori given parameters or on the global error will lead to the automatic shutdown of the refinement procedure unless defining new a posteriori error estimators dedicated to local singularities [24,29,36].

In this paper, we propose geometry-based stopping criteria that enable to automatically turn off the refinement process in case of local singularities in the solution and independently of the considered physical problem. These criteria, independent of the prescribed error, aim to determine the critical region for which the mesh refinement becomes inefficient while respecting the prescribed local accuracy on the remaining part of the domain. Following the idea of the Theory of the Critical Distances in fracture mechanics [40], this critical region can be viewed a discrete volume approximation of the singularity. We provide hence a cheap and easy to implement automatic mesh characterization of the singularity. In the proposed numerical examples, a special attention will be paid on the verification of the prescribed error on the refined mesh.

Multilevel adaptive mesh refinement methods are well designed to deal with local refinement. They consist in sequentially adding local finer meshes in regions of interest. This kind of methodology is cheap because only additional little size problems are solved. Error estimators can be easily coupled to such methods in order to automatically detect the region of interest [5,32]. As the multilevel process is inherently iterative, no density function is required: a fixed refinement ratio can be applied on the detected zones.

Without loss of generality, we will focus in the sequel on linear elastostatics problems with a singular solution due to discontinuous loadings. We will compare the two original refinement automatic geometry-based stopping criteria proposed in this paper with the one based on a minimal number of elements. For this end, the chosen multilevel adaptive mesh refinement method will be the Local Defect Correction (LDC) method [26], well designed for partial differential equations, coupled with a quantitative use of the a posteriori ZZ error estimator [46] on the stress field.

Section 2 is devoted to a brief recall of the multilevel LDC method. The LDC algorithm is written in the case of linear problems. In Sect. 3, the use of a posteriori error estimators in refinement processes is discussed. In this section, two original geometry-based stopping criteria dedicated to automatic mesh refinement in presence of singularities are introduced. Numerical results on examples derived from nuclear engineering are provided in Sect. 4. The ZZ error estimator is used for the automatic refinement process. The efficiency of the proposed strategy is analyzed through the respect of the stress tensor user prescribed tolerances, either in L^2-relative or in L^∞-absolute norm. These results enable to appreciate the performance of the a posteriori-based, fully adaptive multilevel mesh refinement algorithm with automatic stopping criteria in case of singular solutions.

2 Local Defect Correction method for linear problems

The Local Defect Correction method (LDC) [26] is a powerful multilevel adaptive mesh refinement method which is well adapted to finite element discretization of partial differential equations. Local multilevel methods [11] consist in correcting the solution to a problem defined on an initial mesh thanks to an iterative process based on additional local fine meshes resolutions, see Fig. 1. The transfer between the meshes level is based on prolongation and restriction operators as in classical multigrid methods [11,18,27].

The prolongation operator is generic to all the local multilevel adaptive techniques [1,12,26,33]. This operator aims to define Dirichlet boundary conditions on fictive internal fine mesh boundaries from the next coarser mesh, see Fig. 2. The restriction operator, which enables to correct the solution at each level from the next finer mesh, discriminates these various techniques. With the definition of the prolongation operator, energy conservation is ensured and then, unlike the standard multigrid restriction operator, the local multigrid restriction operator has not to be the transpose of the prolongation operator, see [26] for more details.

In the LDC method, the restriction operator is based on the truncation error and consists in defining a defect from the coarse operator applied on the restricted next finer solution.

By extension of the results of [19], the order of the interpolation operators has to be at least the expected order of mesh convergence.

For linear problems, the LDC process involves the iterative resolution of problems $(\mathcal{P}_l^k)$, at iteration k on level l ($0 \leq l \leq l^\star$), written in matrix form (after discretization) in Eq.(1).

$$\begin{cases} [K_l][U_l^k] = [F_l^k] + [N_l] \\ [H_l][U_l^k] = [U_{l,p}^k] + [U_{l,D}] \end{cases} \tag{1}$$

where $[K_l]$ is the stiffness matrix calculated on grid G_l of level l, $[F_l^k]$ is the volume external forces matrix (updated by the restriction operator), $[N_l]$ is the surface external forces matrix (natural Neumann BCs), $[H_l]$ is the Dirichlet boundary conditions discretization matrix, $[U_{l,p}^k]$ is the Dirichlet values derived from the prolongation operation and $[U_{l,D}]$ is the natural Dirichlet BCs values.

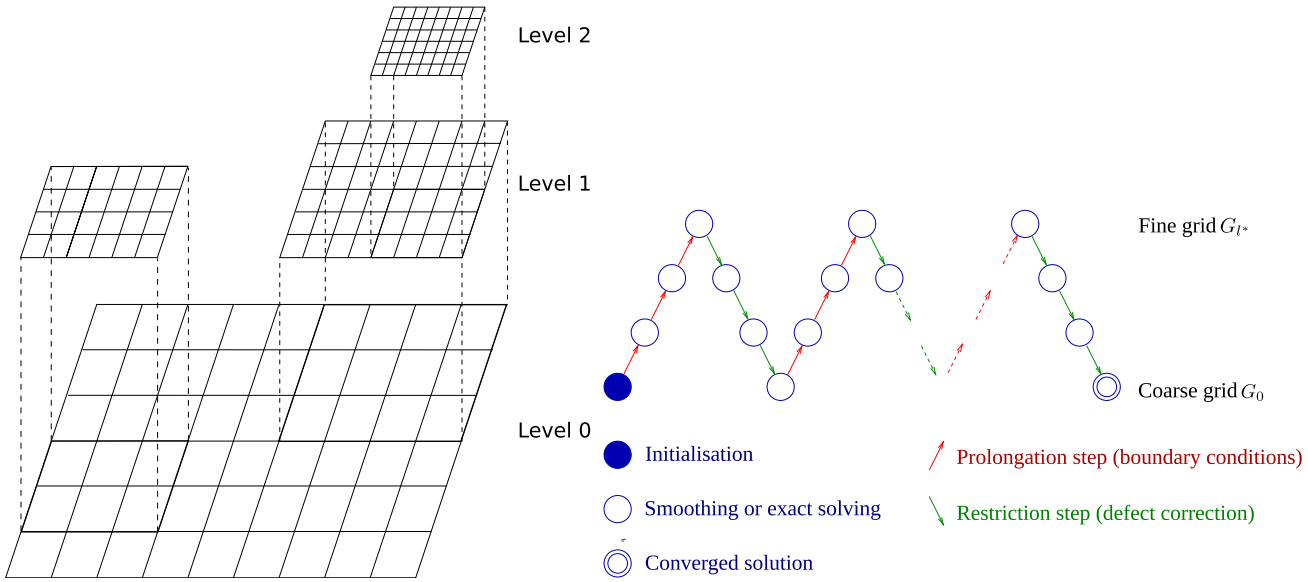

Fig. 1 Local multilevel meshes (left) and process (right)

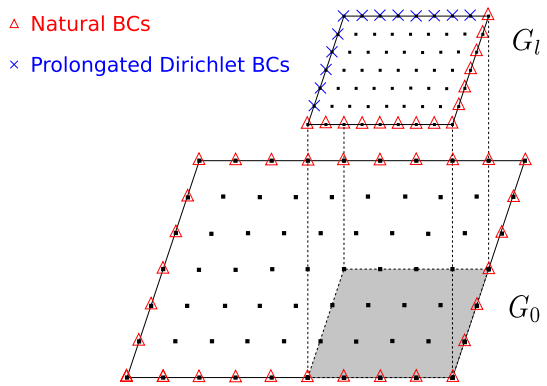

Fig. 2 BCs prolongation in local multilevel processes

Algorithm 1 describes the LDC method for this type of problem. For the sake of simplicity, we denote by ∂G_l the boundary of the domain associated to the grid G_l. The restriction operator slightly differs from the one proposed by Hackbusch [26]. Indeed the subset A_l (and consequently $\mathring{A}_l$) has been enlarged in order to take into account the contribution of the natural BCs on the next finer grid, see [32] for more details.

One can remark that on the initial grid ($k = 0$), only volume forces $[F_0^k]$ are updated during the LDC iterations. Hence, on this grid all boundaries have natural BCs.

One of the main advantage of the LDC method is that it is non-intrusive, only pre- and post-processing operations are made. Existing (industrial) software can hence be used. Moreover, the LDC method is very generic: the solver, the refinement ratio and even the model can change between levels of refinement. This method is very powerful as only low degrees of freedom by level are considered, uniform grids can be used, and stiffness matrix factorizations can be conserved during iterations.

However, prolongation and restriction operators have to be carefully chosen. Their orders have to be in agreement with the expected discretization order. In practice, interpolation operators are used (see Sect. 4.3.2).

This method has been initially introduced and applied for computational fluids problems and has been recently successfully extended to solids mechanics: elastostatics problems in [4], elastostatics problems with frictional contact in [32] and Norton-type material behaviour in [5].

3 On the use of error estimators

In this section, we do not describe error estimators themselves (the reader can refer to [39,42] and the references therein), but their use to detect the zones to be refined. The description of "optimal" mesh design strategies leaning on error estimators is behind the scope of this article (see for example [17] and the reference therein for h-adaptive strategies, especially [14] for mesh design in case of local singularities or stress concentrations).

3.1 Detection of the mesh zones to refine

As said in introduction, the detection of the zones to be refined can be automatically done thanks to an a posteriori error estimator, which gives local estimations $\|e_K\|$ on mesh elements K, with a chosen norm $\|\cdot\|$. Doing this, either a quantitative or a qualitative use of the local error estimator can be proceeded.

Algorithm 1: Multilevel LDC algorithm applied to linear discrete problems

Input: k_{max}: maximal number of iterations, l^* : number of levels of refinement, tol: given tolerance for convergence, G_l: grid at level l, $[K_l]$, $[H_l]$, $[N_l]$, $[U_{l,D}]$: non-iteration-dependent matrices of the discretized linear problem at level l, $[F_l^0]$: initial problem volume forces at level l, $[P_{l-1}^l]$: prolongation operator from grid G_{l-1} to grid G_l ($l = 1, ..., l^*$), $[R_{l+1}^l]$: restriction operator from grid G_{l+1} to grid G_l ($l = l^* - 1, ..., 0$)

Output: $[U_l]$ for $l = 0, ..., l^*$

Initialization: Computation of the initial problem solution $[U_0^0]$ on G_0

$$\begin{cases} [K_0][U_0^0] = [F_0^0] + [N_0] \\ [H_0][U_0^0] = [U_{0,D}] \end{cases}$$

Iterations: Actualization of $[U_l^k]$

for $k=1$ **to** k_{max} **do**

$[U_0^k] = [U_0^{k-1}]$

//Prolongation step//

for $l = 1$ **to** l^* **do**

Prolongated Dirichlet BCs on $\Gamma_l^f = \partial G_l \backslash \partial G_0$

$[U_{l,p}^k] = [P_{l-1}^l][U_{l-1}^k]$

Computation of $[U_l^k]$

$$\begin{cases} [K_l][U_l^k] = [F_l^{k-1}] + [N_l] \\ [H_l][U_l^k] = [U_{l,p}^k] + [U_{l,D}] \end{cases}$$

end

//Restriction step//

for $l = l^* - 1$ **to** 0 **do**

Restriction of the fine grid solution $[U_{l+1}^k]$ **on**

$A_l = \{x \in (G_{l+1} \backslash \Gamma_{l+1}^f) \cap (G_l \backslash \Gamma_l^f)\}$

$[\tilde{U}_l^k] = [R_{l+1}^l][U_{l+1}^k]$ on A_l

Computation of local residual on

$\mathring{A}_l = \{x \in A_l ; [K_l][U_l^1]$ involves only $y \in A_l\}$

$[D_l^k] = [K_l][\tilde{U}_l^k] - [F_l^0]$ on $\mathring{A}_l$

Right-hand side update

$[F_l^k] = [F_l^0] + \chi_{\mathring{A}_l}[D_l^k]$

with $\chi_{\mathring{A}_l}$ the characteristic function of $\mathring{A}_l$: $\chi_{\mathring{A}_l}(x) = \begin{cases} 1 \text{ if } x \in \mathring{A}_l \\ 0 \text{ elsewhere} \end{cases}$

Computation of $[U_l^k]$ **solving**

$$\begin{cases} [K_l][U_l^k] = [F_l^k] + [N_l] \\ [H_l][U_l^k] = [U_{l,p}^k] + [U_{l,D}] \end{cases}$$

end

if $\frac{\|[U_0^k] - [U_0^{k-1}]\|}{\|[U_0^{k-1}]\|} < tol$ **then**

end the algorithm

end

end

The quantitative use simply consists in comparing $\|e_K\|$ to a local user-prescribed tolerance ε and to define the zone Ω_r to be refined as

$$\Omega_r = \{\cup \bar{K};\ K \text{ such that } \|e_K\| > \varepsilon\} \tag{2}$$

with $\bar{K}$ the adherence of K.

If the user tolerance ε is global, the definition of the local error $\|e_K\|$ may lead to multiply the tolerance ε by a (local) coefficient in order to be used for the refined zone detection (2). This coefficient depends on the relation between the local and the global error, see for example [17].

Quantitative approach rests on the reliability of the *a posteriori* error control, or at least the real error overestimation.

On the other hand, the qualitative use of the error estimator is based on a intra-comparison of the local error estimate values. Generally speaking, the refined zone is defined as

$$\Omega_r = \{\cup \bar{K};\ K \text{ such that } \|e_K\| > \alpha \max_L \|e_L\|, \alpha \in [0, 1]\} \tag{3}$$

This qualitative detection is less related to the properties of the error estimator. However, the parameter α is not easy to chose and seems to depend to the problem under study. No simple correlation between the optimum α and expected error levels was found to exist, see [4]. Moreover this estimator needs to be coupled to a stopping criterion in order to avoid an infinite refinement process.

3.2 On the stopping of the refinement process

In this section, we place ourselves in the case of generic error estimators [41], no physically dedicated to singular problems.

When a quantitative estimator is used for refinement zone detection, see Eq. (2), a natural stopping criterion is

$$\Omega_r = \emptyset \tag{4}$$

This stopping criterion is strongly related to the convergence of the local error estimator. In case of singular solutions, defined as solutions that do not converge towards a specific value at a point of the domain (singularity), this stopping criterion can not be used for fine error levels as the usual local error estimator is still growing at the singularity.

In this latter case, additional stopping criteria have to be used. Thank to the Saint Venant's Principle [6], the integral of the solution (even over the singularity region) is not affected by the singularity effect. A global error stopping criterion is then often exploited

$$\|e\| < \varepsilon \tag{5}$$

with e a global error estimate and ε a global user-prescribed tolerance. Here again, this criterion strongly depends on the reliability of the global estimator. The local zone where the user-prescribed error is not respected is often not controlled. This stopping criterion leads to a global optimal mesh (in term of respect of prescribed global accuracy versus minimal number of elements), see [14,31] for example.

A priori stopping criteria can also be used as when qualitative zone detection, see Eq. (3), is employed. Indeed, with a

qualitative detection, Ω_r is never empty. In the literature, one can mainly find the two following *a priori* stopping criteria:

- Fixed number of mesh refinement iterations (see for example [2,5,14,21])
- Minimal number of elements to be refined (see for example [4])

$$NbElt(\Omega_r) \leq NbMin \tag{6}$$

where $NbElt(\Omega_r)$ denotes the number of elements of the detected zone Ω_r and $NbMin$ the prescribed minimal number of elements.

In the first case, no local error is guaranteed. The global real error is generally a posteriori checked and the number of iterations adjusted to reach a desired value for a certain type of problem. If the minimal elements number stopping criterion is combined with a quantitative zone detection, then the local error is controlled outside the stopping region. However, the size of the stopping region may vary with the initial mesh.

3.3 Geometry-based stopping criteria for local singular solution

In this paper, we propose geometry-based a priori stopping criteria that may be useful in case of local adaptive mesh refinement for singular solutions. It relies on the fact that if Ω_r is too small compared to the computation domain Ω, the improvement brought by the new refined mesh will be of low interest. Two geometry-based criteria are proposed here and studied in Sect. 4:

- ratio of mesh measure:

$$|\Omega_r| < \min_{L \in G_0} |L| \tag{7}$$

where $|\cdot|$ denotes the measure and G_0 the initial mesh of Ω. Eq. (7) means that the refinement process is stopped when the measure of the detected refinement zone Ω_r is less than the measure of the smallest element of the initial mesh of Ω. The size of the stopping zone is correlated with the initial grid G_0.
Eventually, this criterion could be extended to n times the measure of any element of G_0.
- ratio of domain measure:

$$|\Omega_r| < \beta |\Omega| \tag{8}$$

with $\beta < 1$.
This criterion expresses that the refinement is turned off when the measure of the zone to be refined is less than a proportion of the computation domain measure. This criterion is independent of the initial grid G_0.

These geometry-based criteria are independent of the prescribed error but they aim to determine the critical region for which the local mesh refinement becomes inefficient. If combined with a quantitative refinement zone detection, the prescribed local accuracy can be respected on the remaining part of the domain as for the minimal number of element criterion. By the way, an automatic mesh characterization of the singularity is provided.

3.4 Combining LDC and error estimators

The genericity of the LDC method (see Sect. 2) enables us to easily combined this method with any error estimator. Hence, the grids G_l are no more inputs of the algorithm, see Algorithm 1, but fully adaptively build during the refinement process.

At each refinement level of the first prolongation step, the error estimator is first applied on the next coarser grid solution in order to detect to potential zone Ω_r to be refined. Then, a stopping criterion is evaluated to decide if Ω_r will give rise to the next local finer grid (with a finer mesh step). If not, the latest refinement level $l^\star$ is reached.

Any choice detection and stopping criteria can be done with the LDC method. In Sect. 4, the three a priori stopping criteria offering a discrete approximation of the singularity (minimal number of elements, ratio of mesh measure and ratio of domain measure) combined with a quantitative detection criterion are compared when being used during the fully adaptive multilevel LDC algorithm.

4 Numerics

4.1 Two numerical examples derived from nuclear engineering studies

In this section, in order to evaluate the strategy presented above, two simplified 2D examples issued from mechanical Pellet-Cladding Interaction (PCI) in nuclear engineering are studied. Even if the singularity is not really strong (see Sect. 4.3.1), these examples are representative of cases where local adaptive mesh refinement won't stop. Moreover, the problem of PCI is essential in this field because the cladding is the first safety enclosure in a pressured water reactor. The contact is very complex due to the various non-linearities involved in the problem: pellet cracking, cladding creep, etc. The aim of this paper is not to analyze PCI in detail but to show the behaviour and effectiveness of the mesh refinement stopping criteria proposed above on simplified PCI models catching the local effects of the pellet-cladding contact. That

Fig. 3 Axisymmetric test case

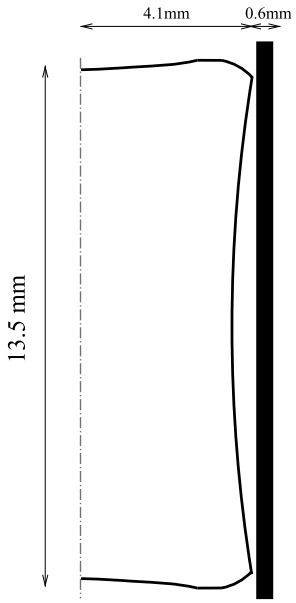

(a) Hourglass shape deformation

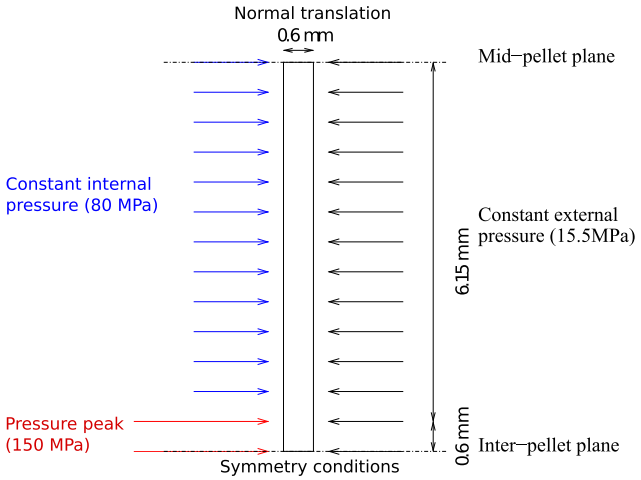

(b) Geometry and loading

is why only the static response of the cladding is studied. The cladding is supposed to be linearly elastic and isotropic with Young's modulus $E = 100$ GPa and Poisson's ratio $\nu = 0,3$. The contact between the pellet and the cladding is modelled by a discontinuous pressure on the internal radius of the cladding. It is obvious that the considered problem lead in elastostatics to a linear system of the form of Eq. (1).

Two 2D tests are represented here (2D axisymmetric and 2D plane strain) in order to study separately two phenomena which are characteristic of the PCI: the hourglass and the fragmentation of the pellet. These test cases have already been proposed in [4].

The hourglass phenomenon is schematically represented by a axisymmetric test case (see Fig. 3). The contact is modelled by a peak of pressure on 600 μm length over the inter-pellet plane. For symmetry reasons, only the half of the pellet is modelled. In order to allow an overall normal displacement of the cladding, a normal (a priori unknown) translation condition is imposed at the mid-pellet plane. In the following, without any analytical solution, comparisons will be made with a very fine reference finite element solution obtained with an uniform mesh step of 2 μm and 1, 053, 801 nodes.

The effect of the pellet cracking on the cladding is represented by a plane strain test case (see Fig. 4). Considering the regularity of the cracks and due to symmetry conditions, only 1/16th of the cladding is considered (see Fig. 4b). The crack opening is supposed to be equal to 8 μm on the internal radius of the cladding. The discontinuous contact betwwen the pellet and the cladding is then modelled by a pressure discontinuity on the cladding. The geometry and the boundary condition are given in Fig. 4b. As for the previous test case, a reference finite element solution, obtained with a quasi-uniform mesh step of 1 μm and 260, 365 nodes, is used for validation purposes.

4.2 An example of error estimate: the Zienkiewicz-Zhu error estimate

There exists a large class of a posteriori error estimates which have been developed for numerous problems: Stokes [34], Maxwell [37], Cracks [10,24,35], Contact [32,44], Coulomb friction [28,30,32], Plasticity [23], Thermal multiphase flows [16], etc. In this paper, we use the first Zienkiewicz and Zhu (ZZ) a posteriori error estimator [45] which is a particular recovery-based error estimator, where a smoothed version of the gradient of displacement or the Cauchy stress tensor is obtained by projection on the base related to the interpolation functions of the discretization method. Then, the ZZ error indicator is given by the difference, in a chosen norm, between the gradient of the approximation (or the Cauchy stress) and the smoothed gradient. In most industrial computational softwares (Abaqus, Aster, etc.), ZZ error estimator family [45–47] had been chosen for its implementation simplicity and its good ratio precision over cost. In the following numerical results, the first ZZ estimator will be coupled with the LDC algorithm without any loss of generality.

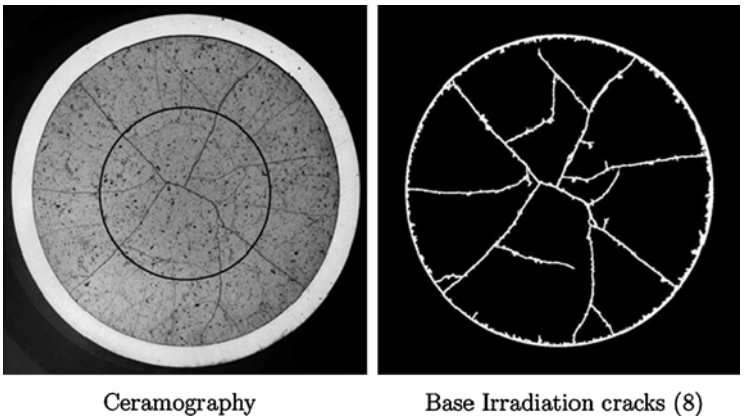

(a) Pellet cracking **(b)** Geometry and loading

Fig. 4 Plane strain test case

4.3 Numerical choices

4.3.1 Finite elements and refinement

In the following section (Sect. 4.4), the two examples presented above (axisymmetric test case and plane strain test case) are discretized using bilinear finite elements (Q1 quadrangular elements). The initial mesh is build to be uniform (or quasi-uniform for the plane strain test case). Hence the position of the pressure discontinuity is approximated by the mesh, *i.e.* on the nearest mesh node. As already shown and studied in [4,38], the convergence rate of the discretization error is of order one in the L^2-norm for the displacement and of order 1/2 for the gradient (here the stress).

The local fine meshes are obtained by dividing each quadrangular element to refine in four quadrangular sub-elements (ratio $r = 2$). It has been shown in [5] that other choices ($r > 2$) are possible.

All the discretized systems take the form of Eq. (1).

4.3.2 Prolongation and restriction operators

The LDC algorithm presented in Sect. 2 needs the use of two operators, one of prolongation and one of restriction, which permit to pass from a level to other one.

To solve the linear problem on grid G_l, it is necessary to define Dirichlet boundary conditions on Γ_l^f (internal fictive boundary) by a prolongation operator. The values of these boundary conditions are obtained by a simple linear interpolation applied to the solution on the closer coarse level U_{l-1}^k. Note, as mentioned in Sect. 2, that the local fine grid has to be enlarged. In our computations the local level is enlarged and structured adding elements in order to obtain quadrangular local grids.

Solution U_l^k is corrected via a residual obtained from the solution on the next finer level U_{l+1}^k. The restriction used here is the canonic one i.e. the value of the displacement on the coarse grid is equal to the value of the displacement on the fine one, for a node common to the two levels. Note that this restriction concerns only the set of nodes not connected with nodes on Γ_l^f in the discretization scheme.

This choice of operators is in agreement with the expected first-order accuracy in displacement of the method.

4.3.3 Error norms

In Sect. 3, it is mentioned that the detection of zones to be refined is linked to a norm that has to be chosen. The relative error in energy norm for the element K can take the following form:

$$\|e_K\|_E = \left(\frac{\int_K (\sigma^* - \sigma_h) : (\epsilon^* - \epsilon_h)\, dK}{\int_K \sigma^* : \epsilon^*\, dK} \right)^{1/2} \tag{9}$$

where σ_h is the stress tensor obtained by the finite elements method, σ^* the ZZ smoothed stress tensor, C fourth order elasticity tensor and $\epsilon_h = C^{-1}\sigma_h, \epsilon^* = C^{-1}\sigma^*$. In order to avoid a zero in the denominator, the following modified energy norm will be preferred

$$\|e_K\|_E = \left(\frac{\int_K (\sigma^* - \sigma_h) : (\epsilon^* - \epsilon_h)\, dK}{\int_K \sigma_h : \epsilon_h\, dK + \int_K (\sigma^* - \sigma_h) : (\epsilon^* - \epsilon_h)\, dK} \right)^{1/2} \tag{10}$$

Lemma 1 *We denote by $\|e_\Omega\|_E$ the error on the composite mesh (sub-level union). Let $\varepsilon > 0$ be given.*

If $\|e_K\|_E \leq \varepsilon$ then $\|e_\Omega\|_E \leq \varepsilon$.

This lemma shows that if the sub-level generation is stopped by $\|e_K\|_E \leq \varepsilon$ with ε given, then $\|e_\Omega\|_E \leq \varepsilon$.

Proof

$$\|e_K\|_E = \left(\frac{\int_K (\sigma^* - \sigma_h) : (\epsilon^* - \epsilon_h)\, dK}{\int_K \sigma_h : \epsilon_h\, dK + \int_K \sigma^* : \epsilon^*\, dK}\right)^{1/2} \leq \varepsilon$$

$$\iff \frac{\int_K (\sigma^* - \sigma_h) : (\epsilon^* - \epsilon_h)\, dK}{\int_K \sigma_h : \epsilon_h\, dK + \int_K \sigma^* : \epsilon^*\, dK} \leq \varepsilon^2$$

$$\iff \int_K (\sigma^* - \sigma_h) : (\epsilon^* - \epsilon_h)\, dK \leq \varepsilon^2 \left(\int_K \sigma_h : \epsilon_h\, dK + \int_K \sigma^* : \epsilon^*\, dK\right)$$

By a sum on the composite grid:

$$\implies \sum_{l=1}^{l^*+1} \sum_{K \subset \Omega_{l-1} \setminus \Omega_l} \int_K (\sigma^* - \sigma_h) : (\epsilon^* - \epsilon_h)\, dK \leq \varepsilon^2 \sum_{l=1}^{l^*+1} \sum_{K \subset \Omega_{l-1} \setminus \Omega_l} \left(\int_K \sigma_h : \epsilon_h\, dK + \int_K \sigma^* : \epsilon^*\, dK\right) \tag{11}$$

with $\Omega_{l^*+1} = \emptyset$.

Thus

$$\|e_\Omega\|_E = \left(\frac{\sum_{l=1}^{l^*+1} \sum_{K \subset \Omega_{l-1} \setminus \Omega_l} \int_K (\sigma^* - \sigma_h) : (\epsilon^* - \epsilon_h)\, dK}{\sum_{l=1}^{l^*+1} \sum_{K \subset \Omega_{l-1} \setminus \Omega_l} \left(\int_K \sigma_h : \epsilon_h\, dK + \int_K \sigma^* : \epsilon^*\, dK\right)}\right)^{1/2} \leq \varepsilon \tag{12}$$

□

In many mechanical problems, the quantity of interest is the well known Von Mises stress. Indeed, this quantity is often required to define the constitutive equations (plasticity, viscoplasticity, etc.). If σ^D denotes the deviatoric part of the stress tensor σ, the Von Mises stress is given by $\sigma^{VM} = \sqrt{\frac{3}{2}\sigma^D : \sigma^D}$. In the following, we consider the absolute error in the infinity norm of the Von Mises stress i.e.

$$\left\|e^{VM}\right\|_\infty = \sup\{\left|\sigma^{*VM} - \sigma_h^{VM}\right|_K ;\ K \in \bigcup_{l=1}^{l*} (\Omega_{l-1} \setminus \Omega_l)\}. \tag{13}$$

Note that in the results presented thereafter this error is computed without taking into account the last level, this could permit to respect the user prescribed tolerance whatever the size of the omitted zone (last level). The geometric criteria permits to this zone to be small and not to depend on the prescribed tolerance in the presence of singularity.

In the sequel, the ZZ estimated errors will be compared to the so-called reference errors, which are equivalent to the real errors where the analytical solution is replaced by the reference solution (defined on a very fine mesh).

4.4 Numerical results

In this section, we perform the multilevel LDC refinement algorithm with a quantitative detection criterion [see Eq. (2)] based on the ZZ estimator, either using the local relative error in energy norm (10) or the local absolute error of the Von Mises stress in infinity norm (13). The two test cases introduced in Sect. 4.1 are used. As these test cases present a local singularity around the point of internal pressure dis-

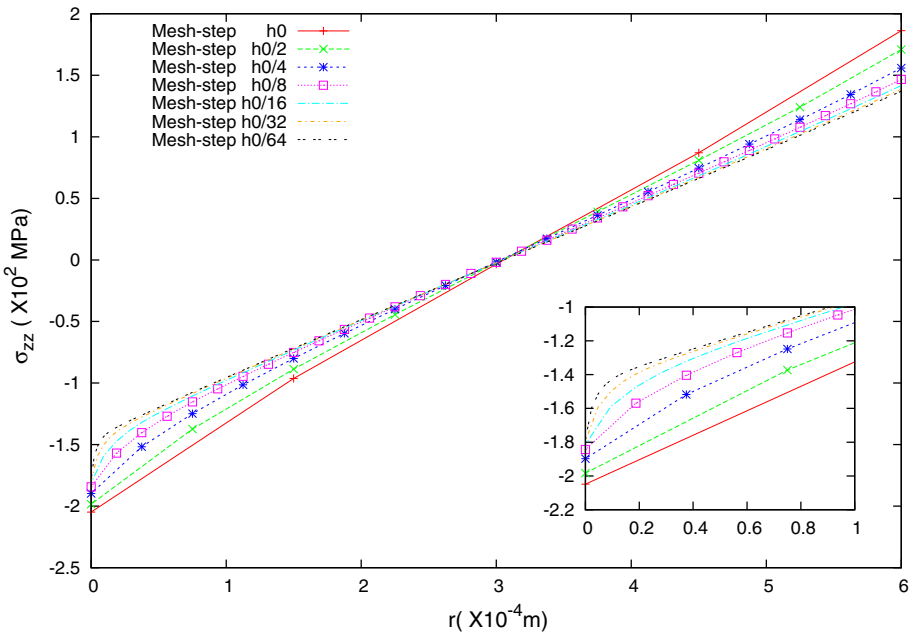

Fig. 5 Axisymmetric test case—Orthoradial stress along the line $z \simeq 600\,\mu$m (defined by the mesh) - $h_0 = 328\,\mu$m

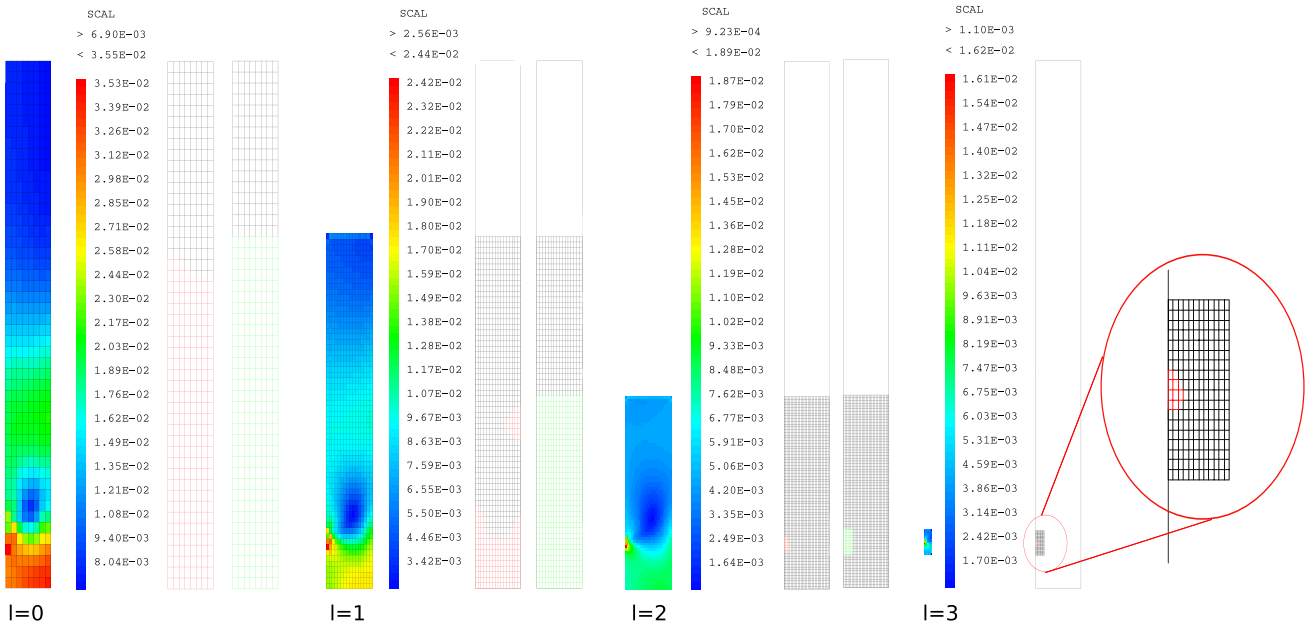

Fig. 6 Axisymmetric test case—example of grid levels obtained for an initial mesh step of 164 μm and $\varepsilon = 1\%$ - ZZ estimator for the relative error in energy norm - Stopping criterion: minimal number of elements (=10)

continuity, see Fig. 5 for example, a stopping criteria for the refinement process is required.

We compare the results obtained for three a priori local stopping criteria: minimal number of elements (Eq. (6)), ratio of mesh measure (Eq. (7)) or ratio of domain measure (Eq. (8)).

The optimal minimal number of elements depends on the test case and will be precised for each of them.

The standard definition of the ratio of mesh measure criterion is used (size of one element of the initial mesh). Preliminary computations indicate that the optimal value of β for the ratio of domain measure criterion is 0.5% independently of the test case. This value is used in the sequel.

4.4.1 Relative error in energy norm

The user-prescribed tolerance ε is a threshold of the relative error in energy norm. Then, the detection criterion writes

$$\|e_K\|_E > \varepsilon$$

with $\|e_K\|_E$ defined by Eq. (10).

Axisymmetric test case For this test case, the optimal minimal number of element for criterion (Eq. (6)) seems to be 10. An example of the obtained grid levels for this stopping criterion is given in Fig. 6.

As expected, the obtained meshes are automatically more and more localized around the pressure discontinuity. The number of DoFs of the finest level is very small (number of DoFs = 247) as can be seen in Table 1. The problems solved by the LDC algorithm at each level have limited size, which lead to an efficient adaptive refinement method. As already mentioned in the literature, we observe than the ZZ estimator underestimates the real error (represented here by the reference error), see Fig. 7.

Tables 1 and 2 enable us to compare the three stopping criteria for two different initial meshes and three user-prescribed thresholds. Complementary results can be found in "Appendix A".

The first conclusion to be drawn is that the refinement process ends whatever the stopping criterion. Secondly, the global user-prescribed tolerance is always reached. This may be due to our local zone detection criterion that is a sufficient but not a necessary condition to respect the global threshold, see Lemma 1. Here, this local detection criterion returns to compensate the ZZ underestimation.

One can obviously conclude that the LDC algorithm is very robust and efficient. The accuracy of the obtained results is directly related to the chosen error estimator and refinement criteria.

Analyzing the two tables, the ratio of domain measure seems the most reliable stopping criterion. The two others criteria have a tendency to over-refine the mesh. Moreover, for the same threshold, the finest refined zone obtained with the ratio of mesh measure criterion is no more coherent as it depends on the initial mesh.

Plane strain test case In this test case, the stress concentrations are more localized, as can be seen in Fig. 8. The minimal number of elements to be refined of criterion (6) had to be changed to 7. Smallest values lead to an infinite refinement

Table 1 Axisymmetric test case—comparison of different stopping criteria for various relative error in energy norm thresholds and an initial mesh step of 164 μm

User-prescribed tolerance		$\varepsilon = 5\%$	$\varepsilon = 2\%$	$\varepsilon = 1\%$
Stopping criterion				
Minimal number of elements (NbMin=10)	$l^\star$ (number of sub-levels generated)	0	1	3
	Number of nodes per grid level	441	441/697	441/1105/2343/247
	Reference relative error	4.20%	2.01%	0.653%
Ratio of mesh measure	$l^\star$	0	1	2
	Number of nodes per grid level	441	441/697	441/1105/2343
	Reference relative error	4.20%	2.01%	0.899%
Ratio of domain measure ($\beta = 0.5\%$)	$l^\star$	0	1	2
	Number of nodes per grid level	441	441/697	441/1105/2343
	Reference relative error	4.20%	2.01%	0.899%

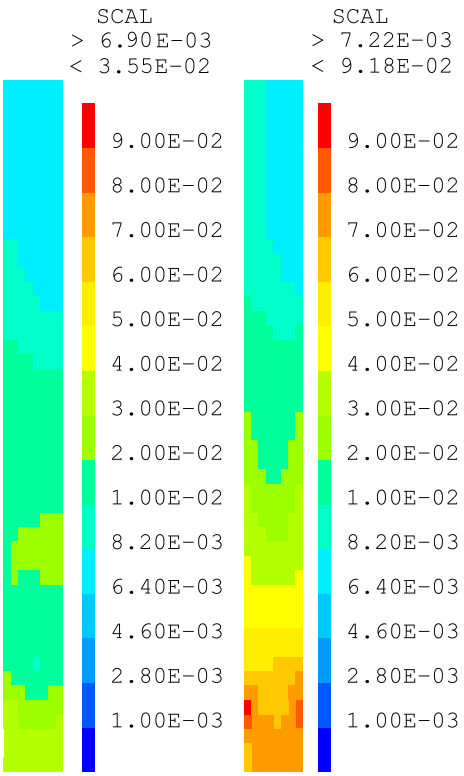

Fig. 7 Axisymmetric test case—comparison between the relative error in energy norm estimated by ZZ (left) and the reference error (right)—legends scaled between 0.1 and 9%—Mesh step 164 μm

process while biggest one turn to no refinement, as confirmed by Fig. 8. This is a main drawback of the minimal number of elements stopping criterion. It had to be filled to each test case.

Tables 3 and 4 summarize some results obtained for the three stopping criteria. Two initial meshes and three user-prescribes tolerances are considered. Complementary results can be found in "Appendix B".

Contrary to the previous test case, the prescribed tolerance is not always reached. This seems to be due to a worst underestimation of the ZZ estimator in this case where the stress discontinuity is very localized, see Fig 8. The local detection criterion is hence not sufficient to compensate this large underestimation. The ratio of mesh measure stopping criterion leads to refinement levels that enable to always respect the prescribed tolerance. However, too much levels are generated, see for example Table 4. The two other stopping criteria lead to slightly exceed the user-given threshold but the refined mesh are coherent whatever the initial mesh. These criteria may be optimal with a more efficient a posteriori error estimator.

Partial conclusion Thanks to the previous results, one can conclude that the LDC algorithm is a efficient adaptive mesh refinement process even in case of local singularity.

The most efficient stopping criterion seems to be the ratio of domain measure (with $\beta = 0.5\%$). It enables to obtain coherent results whatever the initial mesh step. Moreover, it may not depend on the test case and leads to globally respect the prescribed tolerance.

With this stopping criterion, the zone where the prescribed threshold is not locally verified is very small and can be controlled.

4.4.2 Absolute error in infinite norm of the Von Mises stress

In this case, the user-prescribed tolerance ε is a threshold of the absolute Von Mises stress error in the absolute norm. The detection criterion is then

$$\left|e_K^{VM}\right| = \left|\sigma^{*VM} - \sigma_h^{VM}\right|_K > \varepsilon \tag{14}$$

Axisymmetric test case First, we compare on Fig. 9 the estimated and reference absolute errors for the Von Mises

Table 2 Axisymmetric test case—comparison of different stopping criteria for various relative error in energy norm thresholds and an initial mesh step of 82 μm

User-prescribed tolerance		$\varepsilon = 5\%$	$\varepsilon = 2\%$	$\varepsilon = 1\%$
Stopping criterion				
Minimal number of elements (NbMin=10)	$l^\star$ (number of sub-levels generated)	0	0	2
	Number of nodes per grid level	1649	1649	1649/2343/247
	Reference relative error	1.92%	1.92%	0.550%
Ratio of mesh measure	$l^\star$	0	1	2
	Number of nodes per grid level	1649	1649/117	1649/2343/247
	Reference relative error	1.92%	1.01%	0.550%
Ratio of domain measure ($\beta = 0.5\%$)	$l^\star$	0	0	1
	Number of nodes per grid level	1649	1649	1649/2343
	Reference relative error	1.92%	1.92%	0.83%

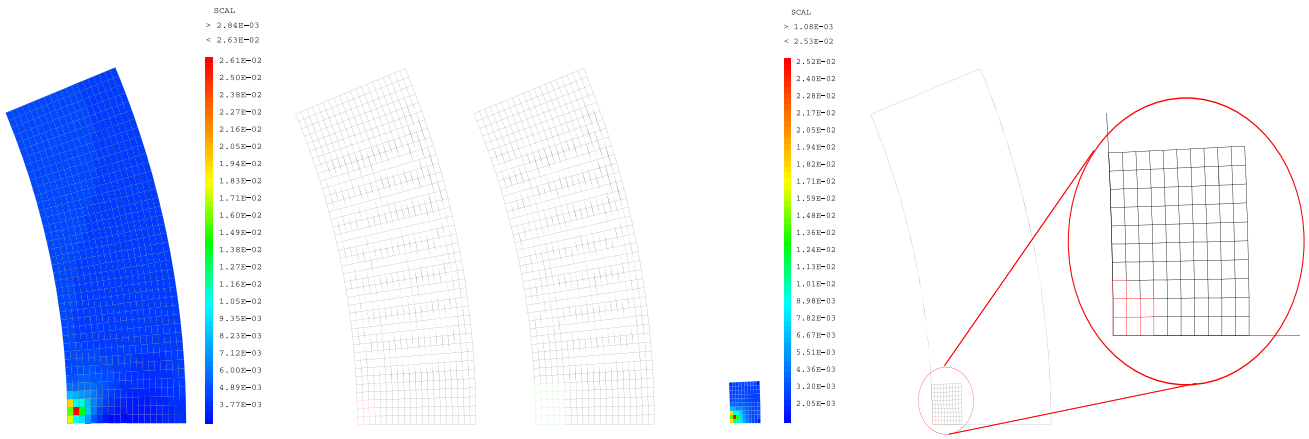

Fig. 8 Plane strain test case—example of grid levels obtained for an initial mesh step of 54.5 μm and $\varepsilon = 1\%$—ZZ estimator for the relative error in energy norm—stopping criterion: minimal number of elements (=7)

Table 3 Plane strain test case—comparison of different stopping criteria for various relative error in energy norm thresholds and an initial mesh step of 54.5 μm

User-prescribed tolerance		$\varepsilon = 5\%$	$\varepsilon = 2\%$	$\varepsilon = 1\%$
Stopping criterion				
Minimal number of elements (NbMin=7)	$l^\star$(number of sub-levels generated)	0	0	1
	Number of nodes per grid level	861	861	861/121
	Reference relative error	3.19%	3.19%	1.27%
Ratio of mesh measure	$l^\star$	0	1	2
	Number of nodes per grid level	861	861/81	861/121/121
	Reference relative error	3.19%	1.27%	0.462%
Ratio of domain measure ($\beta = 0.5\%$)	$l^\star$	0	0	1
	Number of nodes per grid level	861	861	861/121
	Reference relative error	3.19%	3.19%	1.27%

stress. We can conclude that the ZZ estimator well approximates the Von Mises stress with still a little underestimation of large errors. In Table 5, we report various calculations made for different thresholds and initial meshes. The reference absolute error is also mentioned. The first conclusion to be drawn is that the user-prescribed tolerance is glob-

Table 4 Plane strain test case—comparison of different stopping criteria for various relative error in energy norm thresholds and an initial mesh step of 27.25 μm

User-prescribed tolerance		$\varepsilon = 5\%$	$\varepsilon = 2\%$	$\varepsilon = 1\%$
Stopping criterion				
Minimal number of elements (NbMin=7)	$l^\star$(number of sub-levels generated)	0	0	0
	Number of nodes per grid level	3321	3321	3321
	Reference relative error	1.22%	1.22%	1.22%
Ratio of mesh measure	$l^\star$	0	1	2
	Number of nodes per grid level	3321	3321/81	3321/121/121
	Reference relative error	1.22%	0.294%	0.289%
Ratio of domain measure ($\beta = 0.5\%$)	$l^\star$	0	0	0
	Number of nodes per grid level	3321	3321	3321
	Reference relative error	1.22%	1.22%	1.22%

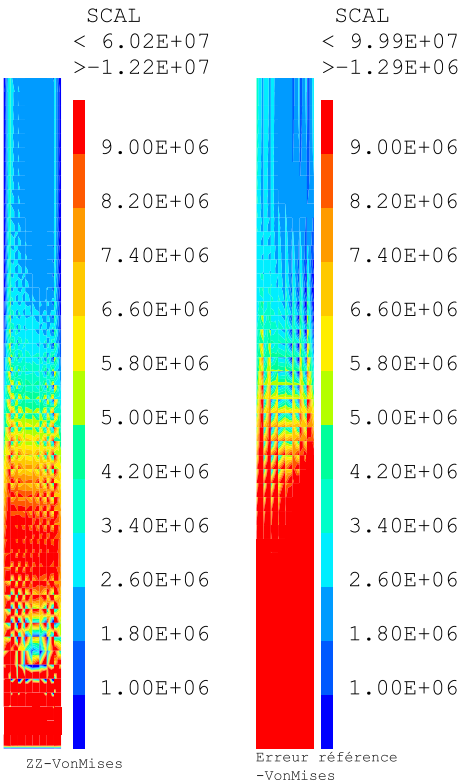

Fig. 9 Axisymmetric test case—comparison between the Von Mises stress absolute error in infinite norm estimated by ZZ (left) and the reference error (right)—legend scaled between 1 10^6 and 9 10^6—mesh step 164 μm

ally well respected. This confirms that the multilevel LDC algorithm is very efficient and robust whatever the kind of prescribed error (relative or absolute) and that the accuracy of the obtained results is only related to the error estimator used. The underestimation of the ZZ estimator tends to a little excess of the fine user-prescribed tolerances (see for example the row $\varepsilon = 2$ MPa). As for the relative error test cases, the number and the size of refinement levels automatically generated by the LDC algorithm are coherent between different initial mesh steps (see rows of Table 5). Moreover, the more the user-prescribed threshold is little, the more the number and the size of the refined levels are big (see lines of Table 5). Finally, thanks to the ratio of domain measure stopping criterion, the finest grid zone where the absolute error threshold is not respected remains small and localized.

Plane strain test case For this second test case, the proposed strategy has also been applied to respect an absolute error tolerance. The results are reported in Table 6. The user-prescribed thresholds are well respected. It is interesting to remark that in this case, in order to reach finer thresholds (see lines of Table 6), the proposed algorithm tends to enlarge the refined zones instead to add additional levels. However, it seems that for the largest threshold ($\varepsilon = 10$ MPa), too much sub-levels are generated.

We then reported in Table 7, the reference absolute errors when the number of sub-levels are a priori fixed. We can conclude that the number of automatically generated sub-levels (see Table 6) is congruent with the desired threshold. However, one level less of refinement would still lead to satisfactory results. For example, in a case of an initial mesh of 109 μm, 2 levels of refinement lead to an error of 10.63 MPa which is greater but very close to the desired threshold of 10 MPa.

Partial conclusion The LDC algorithm combined with the proposed stopping criteria based on a ratio of the domain measure turns out to be a really efficient adaptive mesh refinement algorithm even for absolute errors in infinite norm thresholds. This kind of thresholds are rarely (maybe never) studied in the literature. However, as already mentioned in Sect. 4.3.3 the infinite norm of the Von Mises stress absolute error is of great interest for engineering studies.

Table 5 Axisymmetric test case—absolute Von Mises stress error in infinite norm thresholds—stopping criteria: ratio of domain measure ($\beta = 0.5$ %)

User-prescribed tolerance		$\varepsilon = 10\,MPa$	$\varepsilon = 5\,MPa$	$\varepsilon = 2\,MPa$
Initial mesh step				
328 μm	$l^\star$ (number of sub-levels generated)	4	5	6
	Number of nodes per grid level	125/297/697/891/285	125/441/1071/2541/2925/621	125/441/1649/4653/11895/12513/38293
	Reference absolute error	8.34 MPa	5.00 MPa	2.25 MPa
164 μm	$l^\star$	3	4	5
	Number of nodes per grid level	441/697/891/285	441/1071/2541/2925/621	441/1649/4653/11895/12513/38239
	Reference absolute error	8.32 MPa	5.00 MPa	2.25 MPa
82 μm	$l^\star$	2	3	4
	Number of nodes per grid level	1649/891/315	1649/2541/2925/621	1649/4653/11895/12513/38239
	Reference absolute error	8.28 MPa	4.99 MPa	2.25 MPa
41 μm	$l^\star$	1	2	3
	Number of nodes per grid level	6369/315	6369/2925/621	6369/11895/12513/38239
	Reference absolute error	8.29 MPa	4.99 MPa	2.25 MPa

Table 6 Plane strain test case—absolute Von Mises stress reference error in infinite norm thresholds—stopping criteria: ratio of domain measure ($\beta = 0.5\%$)

User-prescribed tolerance		$\varepsilon = 10\,MPa$	$\varepsilon = 5\,MPa$	$\varepsilon = 2MPa$
Initial mesh step				
109 μm	$l^\star$ (number of sub-levels generated)	3	3	3
	Number of nodes per grid level	231/99/99/99	231/861/143/169	231/861/3321/289
	Reference absolute error	4.45 MPa	3.35 MPa	2.06 MPa
54.5 μm	$l^\star$	2	2	2
	Number of nodes per grid level	861/99/99	861/143/169	861/3321/289
	Reference absolute error	2.97 MPa	2.80 MPa	2.06 MPa
27.25 μm	$l^\star$	1	1	1
	Number of nodes per grid level	3321/99	3321/143	3321/289
	Reference absolute error	3.04 MPa	2.62 MPa	2.06 MPa

Table 7 Plane strain test case—absolute Von Mises stress errors in infinite norm for $\varepsilon = 10$ MPa and various number of sub-levels—stopping criteria: ratio of domain measure ($\beta = 0.5\%$)

l* (maximal number of sub-levels)	1	2	3
Initial mesh step			
109 μm	25.73 MPa	10.63 MPa	4.45 MPa
54.5 μm	10.44 MPa	2.97 MPa	
27.25 μm	3.04 MPa		

5 Conclusions and perspectives

In this paper, we have introduced two new geometry-based stopping criteria in the context of automatic adaptive mesh refinement. These criteria are especially useful in case of singular solutions to avoid an infinite refinement process. They consist in automatically determining a discrete volume approximation of the singularity where the local refinement is inefficient. Even if in this zone the local error is no more controlled, the global accuracy is still respected. The first criterion is based on a ratio of a mesh measure between the initial mesh of the computation domain and the detected zone to be refined. This criterion works well but as it depends on the initial mesh, it can lead to over-refine the mesh. The second criterion is more mesh-independent and consists in a domain measure ratio between the computation domain and the detected zone to be refined. With these two criteria, we can a priori control the zone where the local user-prescribed tolerance is unreached.

These two stopping criteria have been combined with an efficient multilevel algorithm (Local Defect Correction method) through a classical a posteriori error estimator (Zienkiewicz and Zhu). The proposed strategy turns out to give very satisfactory results compared to a more basic stopping criterion based on a minimal number of elements. In particular, the proposed ratio of domain stopping criterion automatically determines the critical region where the refinement becomes inefficient. Our strategy succeeds to reach user-prescribed tolerance for relative error in energy norm as well as for absolute Von Mises error in infinite norm. The latter case, poorly studied in the literature, is of great interest for engineering applications.

Further works will concern the use of these new stopping criteria in the framework of others adaptive mesh refinement techniques such as the well-known h-adaptive refinement methods. Then, we could compare the efficiency of the different mesh-step refinement strategies (multilevel or recursive h-methods) to deal with singular solutions.

Acknowledgements This work has been achieved in the framework of the collaboration protocol between the CEA (Commissariat à l'Énergie Atomique et aux Énergies Alternatives) and the LMA (Laboratoire de Mécanique et d'Acoustique, CNRS, Marseille). The authors are grateful to the PLEIADES project, financially supported by CEA, EDF (Électricité de France) and AREVA, that funded this research work.

A Extended results for the axisymmetric test case

See Tables 8, 9 and 10.

Table 8 Axisymmetric test case—relative error in energy norm thresholds—stopping criteria: minimal number of elements (NbMin = 10)

User-prescribed tolerance		$\varepsilon = 5\%$	$\varepsilon = 2\%$	$\varepsilon = 1\%$
Initial mesh step				
328 μm	$l^\star$ (number of sub-levels generated)	1	2	4
	Number of nodes per grid level	125/99	125/315/697	125/441/1105/2343/247
	Reference relative error	4.84%	2.11%	0.653%
164 μm	$l^\star$	0	1	3
	Number of nodes per grid level	441	441/697	441/1105/2343/247
	Reference relative error	4.20%	2.01%	0.653%
82 μm	$l^\star$	0	0	2
	Number of nodes per grid level	1649	1649	1649/2343/247
	Reference relative error	1.92%	1.92%	0.550%
41 μm	$l^\star$	0	0	1
	Number of nodes per grid level	6369	6369	6369/247
	Reference relative error	0.757%	0.757%	0.443%

Table 9 Axisymmetric test case—relative error in energy norm thresholds—stopping criteria: ratio of mesh measure

User-prescribed tolerance		$\varepsilon = 5\%$	$\varepsilon = 2\%$	$\varepsilon = 1\%$
Initial mesh step				
328 μm	$l^\star$ (number of sub-levels generated)	1	2	3
	Number of nodes per grid level	125/99	125/315/697	125/441/1105/2343
	Reference relative error	4.84%	2.11%	0.899%
164 μm	$l^\star$	0	1	2
	Number of nodes per grid level	441	441/697	441/1105/2343
	Reference relative error	4.20%	2.01%	0.899%
82 μm	$l^\star$	0	1	2
	Number of nodes per grid level	1649	1649/117	1649/2343/247
	Reference relative error	1.92%	1.01%	0.550%
41 μm	$l^\star$	0	0	2
	Number of nodes per grid level	6369	6369	6369/247/187
	Reference relative error	0.757%	0.757%	0.440%

Table 10 Axisymmetric test case—relative error in energy norm thresholds—stopping criteria: ratio of domain measure ($\beta = 0.5\%$)

User-prescribed tolerance		$\varepsilon = 5\%$	$\varepsilon = 2\%$	$\varepsilon = 1\%$
Initial mesh step				
328 μm	$l^\star$ (number of sub-levels generated)	1	2	3
	Number of nodes per grid level	125/99	125/315/697	125/441/1105/2343
	Reference relative error	4.84%	2.11%	0.899%
164 μm	$l^\star$	0	1	2
	Number of nodes per grid level	441	441/697	441/1105/2343
	Reference relative error	4.20%	2.01%	0.899%
82 μm	$l^\star$	0	0	1
	Number of nodes per grid level	1649	1649	1649/2343
	Reference relative error	1.92%	1.92%	0.83%
41 μm	$l^\star$	0	0	0
	Number of nodes per grid level	6369	6369	6369
	Reference relative error	0.757%	0.757%	0.757%

B Extended results for the plane strain test case

See Tables 11, 12 and 13.

Table 11 Plane strain test case—relative error in energy norm thresholds—stopping criteria: minimal number of elements (NbMin = 7)

User-prescribed tolerance		$\varepsilon = 5\%$	$\varepsilon = 2\%$	$\varepsilon = 1\%$
Initial mesh step				
109 μm	$l^\star$ (number of sub-levels generated)	0	0	2
	Number of nodes per grid level	231	231	231/861/121
	Reference relative error	7.05%	7.05%	1.27%
54.5 μm	$l^\star$	0	0	1
	Number of nodes per grid level	861	861	861/121
	Reference relative error	3.19%	3.19%	1.27%
27.25 μm	$l^\star$	0	0	0
	Number of nodes per grid level	3321	3321	3321
	Reference relative error	1.22%	1.22%	1.22%

Table 12 Plane strain test case—relative error in energy norm thresholds—stopping criteria: ratio of mesh measure

User-prescribed tolerance		$\varepsilon = 5\%$	$\varepsilon = 2\%$	$\varepsilon = 1\%$
Initial mesh step				
109 μm	$l^\star$ (number of sub-levels generated)	0	1	2
	Number of nodes per grid level	231	231/99	231/861/121
	Reference relative error	7.05%	3.28%	1.27%
54.5 μm	$l^\star$	0	1	2
	Number of nodes per grid level	861	861/81	861/121/121
	Reference relative error	3.19%	1.27%	0.462%
27.25 μm	$l^\star$	0	1	2
	Number of nodes per grid level	3321	3321/81	3321/121/121
	Reference relative error	1.22%	0.294%	0.289%

Table 13 Plane strain test case—relative error in energy norm thresholds—stopping criteria: ratio of domain measure ($\beta = 0.5\%$)

User-prescribed tolerance		$\varepsilon = 5\%$	$\varepsilon = 2\%$	$\varepsilon = 1\%$
Initial mesh step				
109 μm	$l^\star$ (number of sub-levels generated)	0	1	2
	Number of nodes per grid level	231	231/99	231/861/121
	Reference relative error	7.05%	3.28%	1.27%
54.5 μm	$l^\star$	0	0	1
	Number of nodes per grid level	861	861	861/121
	Reference relative error	3.19%	3.19%	1.27%
27.25 μm	$l^\star$	0	0	0
	Number of nodes per grid level	3321	3321	3321
	Reference relative error	1.22%	1.22%	1.22%

References

1. Angot P, Caltagirone J, Khadra K (1992) Une méthode adaptative de raffinement local : la Correction de Flux à l'Interface. CR de l'Académie des Sci de Paris 315:739–745
2. Bank R, Sherman A, Weiser A (1983) Some refinement algorithms and data structures for regular local mesh refinement. Sci Comput Appl Math Comput Phys Sci 1:3–17
3. Bank R, Weiser A (1985) Some a posteriori error estimators for elliptic partial differential equations. Math Comput 44(170):283–301
4. Barbié L, Ramière I, Lebon F (2014) Strategies around the local defect correction multi-level refinement method for three-dimensional linear elastic problems. Comput Struct 130:73–90
5. Barbié L, Ramière I, Lebon F (2015) An automatic multilevel refinement technique based on nested local meshes for nonlinear mechanics. Comput Struct 147:14–25
6. Barré de Saint-Venant AJC (1855) Mémoire sur la torsion des prismes. Mémoires présentés par divers savants. Acad Sci 14:233–560
7. Bellenger E, Coorevits P (2005) Adaptive mesh refinement for the control of cost and quality in finite element analysis. Finite Elem Anal Des 41(15):1413–1440
8. Berger M, Colella P (1989) Local adaptive mesh refinement for shock hydrodynamics. J Comput Phys 82:64–84
9. Biotteau E, Gravouil A, Lubrecht A, Combescure A (2012) Three dimensional automatic refinement method for transient small strain elastoplastic finite element computations. Comput Mech 49(1):123–136
10. Bordas S, Duflot M, Le P (2007) A simple error estimator for extended finite elements. Commun Numer Methods Eng 24(11):961–971. https://doi.org/10.1002/cnm.1001
11. Brandt A (1977) Multi-level adaptive solutions to boundary-value problems. Math Comput 31:333–390
12. Brandt A (1994) Rigorous quantitative-analysis of multigrid.1. constant-coefficients 2-level cycle with l2-norm. SIAM J Numer Anal 31(6):1695–1730
13. Coorevits P, Hild P, Pelle J (2000) A posteriori error estimation for unilateral contact with matching and non-matching meshes. Comput Methods Appl Mech Eng 186(1):65–83
14. Coorevits P, Ladevèze P, Pelle JP (1995) An automatic procedure with a control of accuracy for finite element analysis in 2D elasticity. Comput Methods Appl Mech Eng 121(1):91–120
15. Demkowicz L, Devloo P, Oden J (1985) On a h-type mesh-refinement strategy based on minimization of interpolation errors. Comput Methods Appl Mech Eng 53(1):67–89
16. Di Pietro DA, Vohralik M, Yousef S (2014) An a posteriori-based, fully adaptive algorithm with adaptive stopping criteria and mesh refinement for thermal multiphase compositional flows in porous media. Comput Math Appl 68(12, Part B):2331–2347. https://doi.org/10.1016/j.camwa.2014.08.008
17. Ehlers W, Ammann M, Diebels S (2002) h-adaptive fe methods applied to single-and multiphase problems. Int J Numer Methods Eng 54(2):219–239
18. Fedorenko R (1961) A relaxation method for solving elliptic difference equations. USSR Comput Math Math Phys 1:1092–1096
19. Ferket P, Reusken A (1996) Further analysis of the local defect correction method. Computing 56(2):117–139
20. Fish J, Markolefas S (1994) Adaptive global-local refinement strategy based on the interior error-estimatesd of the h-method. Int J Numer Methods Eng 37(5):827–838
21. Fournier D, Herbin R, Tellier RL (2013) Discontinuous Galerkin discretization and hp-refinement for the resolution of the neutron transport equation. SIAM J Sci Comput 35(2):A936–A956. https://doi.org/10.1137/110844581
22. Gallimard L, Ladevèze P, Pelle J (1996) Error estimation and adaptivity in elastoplasticity. Int J Numer Methods Eng 39:189–217
23. Gallimard L, Ladevèze P, Pelle J (2000) An enhanced error estimator on the constitutive relation for plasticity problems. Comput Struct 78:801–810
24. Gerasimov T, Rüter M, Stein E (2012) An explicit residual-type error estimator for Q1-quadrilateral extended finite element method in two-dimensional linear elastic fracture mechanics. Int J Numer Methods Eng 90(9):1118–1155
25. Guo B, Babuška I (1986) The hp version of the finite element method. Comput Mech 1(1):21–41
26. Hackbusch W (1984) Local defect correction method and domain decomposition techniques, vol 5. Computing suppl. Springer, Berlin, pp 89–113
27. Hackbusch W (1985) Multi-grid methods and applications, vol 4. Springer series in computational mathematics. Springer, Berlin
28. Hild P, Lleras V (2009) Residual error estimates for coulomb friction. SIAM J Numer Anal 47(5):3550–3583
29. Hugger J (1994) An asymptotically exact, pointwise, a posteriori error estimator for linear, elliptic, one-dimensional problems with possible singularities in the solution. J Comput Appl Math 54(2):185–220
30. Kuss F, Lebon F (2011) Error estimation and mesh adaptation for Signorini-Coulomb problems using E-FEM. Comput Struct 89(11–12):1148–1154
31. Ladevèze P, Pelle J, Rougeot P (1991) Error estimation and mesh optimization for classical finite elements. Eng Comput 8(1):69–80
32. Liu H, Ramière I, Lebon F (2017) On the coupling of local multilevel mesh refinement and ZZ methods for unilateral frictional

contact problems in elastostatics. Comput Methods Appl Mech Eng 323:1–26
33. McCormick S (1984) Fast adaptive composite grid (F.A.C.) methods : theory for the variational case, vol 5. Computing suppl. Springer, Berlin, pp 115–121
34. Oden J, Wu W, Ainsworth M (1994) An a posteriori error estimate for finite element approximations of the navier-stokes equations. Comput Methods Appl Mech Eng 111(1–2):185–202
35. Pares N, Díez P, Huerta A (2006) Subdomain-based flux-free a posteriori error estimators. Comput Methods Appl Mech Eng 195:297–323
36. Petzoldt M (2002) A posteriori error estimators for elliptic equations with discontinuous coefficients. Adv Comput Math 16(1):47–75. https://doi.org/10.1023/A:1014221125034
37. Rachowicz W, Zdunek A (2005) An hp-adaptive finite element method for scattering problems in computational electromagnetics. Int J Numer Methods Eng 62(9):1226–1249
38. Ramière I (2008) Convergence analysis of the Q_1-finite element method for elliptic problems with non-boundary-fitted meshes. Int J Numer Methods Eng 75(9):1007–1052
39. Segeth K (2010) A review of some a posteriori error estimates for adaptive finite element methods. In: ESCO 2008 conference mathematics and computers in simulation, vol 80(8), pp 1589–1600
40. Taylor D (2007) The theory of critical distances : a new perspectives in fracture mechanics. Elsevier, Oxford
41. Verfürth R (1989) A posteriori error estimators for the stokes equations. Numer Math 55(3):309–325. https://doi.org/10.1007/BF01390056
42. Verfürth R (1996) A review of a posteriori error estimation and adaptive mesh-refinement techniques. Wiley, Hoboken
43. Verfürth R (1999) A review of a posteriori error estimation techniques for elasticity problems. Comput Methods Appl Mech Eng 176(1):419–440
44. Wriggers P, Scherf O (1998) Different a posteriori error estimators and indicators for contact problems. Math Comput Model 28(4–8):437–447
45. Zienkiewicz O, Zhu J (1987) A simple error estimator and adaptive procedure for practical engineering analysis. Int J Numer Methods Eng 24:337–357
46. Zienkiewicz O, Zhu J (1992) The superconvergent patch recovery and a posteriori error estimation. Part I: The recovery technique. Int J Numer Methods Eng 33:1331–1364
47. Zienkiewicz O, Zhu J (1992) The superconvergent patch recovery and a posteriori error estimation. Part II: Error estimates and adaptivity. Int J Numer Methods Eng 33:1365–1382